



## Self-adaptive medium access control protocol for aggregated VLC–RF wireless networks

K. Küçük <sup>a,\*</sup>, D.L. Msongaleli <sup>a</sup>, O. Akbulut <sup>a</sup>, A. Kavak <sup>a</sup>, C. Bayılmış <sup>b</sup>

<sup>a</sup> Department of Computer Engineering, Kocaeli University, Umuttepe Campus, 41001, Izmit/Kocaeli, Turkey

<sup>b</sup> Department of Computer Engineering, Sakarya University, Esentepe Campus, 54050, Serdivan/Sakarya, Turkey



### ARTICLE INFO

**Keywords:**

VLC  
WiFi  
MAC  
Markov chain  
IEEE 802.15.7  
VLC-RF

### ABSTRACT

Visible light communication (VLC) is an emerging technology that uses light rays in the range of 380–740 nm for signal propagation at a high data rate compared to radio frequency (RF). Nevertheless, it is not realistic to achieve full-duplex communication in VLC because of challenges such as glare, line-of-sight transmission requirement, interference, and energy constraint. Infrared or RF can complement VLC in order to achieve full-duplex communication. However, aggregated VLC–RF networks cannot be realized without addressing challenges such as network addressing and medium access control (MAC). In this study, we present the self-adaptive medium access control (SA-MAC) protocol for aggregated VLC–RF wireless networks. The aim of our study is to minimize network delay, energy consumption, and collision while increasing throughput. By leveraging the CSMA/CA and sub-carrier orthogonality we model the SA-MAC protocol for aggregated VLC–RF wireless networks and we demonstrate the discrete Markov chain model that shows the states of a node in SA-MAC. Finally, we simulate our protocol in NS3 simulator then we compare simulation results with the Markov chain results and other existing protocols in the literature such as the carrier sense multiple access with collision detection hidden node avoidance (CSMA/CD-HA) and dynamic contention window-based successive transmission (DCW-ST). Numerical results from simulation and Markov chain model converge, especially when the number of node increases. Furthermore, the results from our study show that the proposed protocol increases network performance significantly.

### 1. Introduction

The profound reliance on the internet is a challenge facing the internet industry. Currently, the majority of wireless internet traffic relies on radio spectrum. Accordingly, the radio spectrum is almost exhausted and adding new subscribers reveals emergent problems. The visible light spectrum is a potential solution to the ever-increasing bandwidth demand. The motivating factors of using visible light communication (VLC) include; visible light spectrum is unlicensed, many potential available channel, immune to electromagnetic interference, not harmful to human being, rapid establishment and security. The IEEE has introduced the IEEE 802.15.7 standard in order to standardize short range optical wireless communications such as VLC. The IEEE 802.15.7 standard specifies several issues such as collision avoidance, addressing, network topologies, visibility support, dimming support, and acknowledgement [1]. In terms of network topologies, the standard proposes star, broadcast, and peer-to-peer topologies. In addition, the IEEE 802.15.7 standard specifies the physical layer and the medium access control (MAC) techniques.

Several challenges need to be addressed in order to realize potential benefits of VLC technology. These challenges are inter-cell interference, backbone network design, uplink and multi-user MAC design, and network addressing problem [2,3]. Most of the researches in VLC focus on the downlink channel. There is little attention on the uplink channel in VLC networks. Achieving full-duplex communication in VLC standalone system is not realistic unless it is complemented by Infrared or radio frequency (RF) for the uplink channel because of energy constraints for mobile nodes. Hybrid and aggregated VLC–RF systems have been proposed in the literature as the best way to achieve full-duplex communication in VLC networks [3–7].

Despite the benefits of visible light spectrum, VLC standalone systems cannot provide full-duplex communication considering constraints such as interference, glare, and power consumption. Accordingly, the use of infrared or radio frequency (RF) to complement VLC in order to achieve full-duplex communication has been demonstrated in [2,3]. The realization of aggregated wireless networks such as VLC–RF and Infrared-VLC requires mitigating challenges such as network addressing techniques, MAC techniques, etc. For instance, in this type of networks each node is enabled with two network interface cards (NICs) in order

\* Corresponding author.

E-mail address: [kkucuk@kocaeli.edu.tr](mailto:kkucuk@kocaeli.edu.tr) (K. Küçük).

**Table 1**  
List of abbreviations.

ACK	Acknowledgement Frame
AP	Access Point
BC	Beacon
BE	Beacon Exponents
CAP	Contention Access Period
CCA	Clear Channel Assessment
CFP	Contention Free Period
CU	Control-Unit
CSMA	Carrier Sense Multiple Access
CSMA/CA	CSMA with Collision Avoidance
CSMA/CD-HA	CSMA with Collision Detection Hidden node Avoidance
CTS	Clear-to-Send Frame
DC	Direct Current
DCW-ST	Dynamic Contention Window-based Successive Transmission
DFK	Dynamic Future Knowledge
DTF	Data Transmission Frame
LED	Light Emitting Diode
MAC	Medium Access Control
MTU	Maximum Transmission Unit
NICs	Network Interface Cards
NS3	Network Simulator 3
OFDMA	Orthogonal Frequency Division Multiple Access
PDs	Photodiodes
PT	Polling Table
PT-MAC	Parallel Transmission-MAC
RF	Radio Frequency
RTT	Round Trip Time
RTS	Request-to-Send Frame
SA-MAC	Self-Adaptive Medium Access Control
VLC	Visible Light Communication
VLC-RF	Visible Light Communication-Radio Frequency
WiFi	Wireless Fidelity
WiFi-VLC	Wireless Fidelity-Visible Light Communication

to receive and transmit both radio and visible light signals. These devices work together to accomplish full-duplex communication. This is a challenge in terms of MAC and network addressing perspectives. Traditional MAC protocols consider as NIC for each device that serves for both the uplink and downlink channel. Therefore, it is imperative to design a novel MAC protocol that takes into consideration these challenges.

In this study, we present the self-adaptive medium access control (SA-MAC) protocol for aggregated VLC-RF wireless networks wherein the objectives are maximizing network throughput while minimizing energy consumption, delay, and collision. Self-adaptive, in here, corresponds to dynamic superframe size, which depends on the number of nodes in the network. In other words, we propose dynamically adjusts the size of the superframe and the size of the maximum transmission unit (MTU) depending on the number of nodes in the polling table (PT). By periodically adjusting the dynamic future knowledge (DFK) MTU and the size of the superframe, our protocol minimizes non-transmission time in each superframe and improves the overall performance of the system. The discrete Markov chain model is also presented in order to show the validity of our protocol. The simulation of the proposed protocol is performed by using the NS3 discrete event network simulator. Numerical results for both simulation and the Markov chain model converge especially when number of node increases.

The rest of this study is organized as follows: The literature review is presented in Section 1.1, in Section 2 we provide details of the problem we address, detailed description of the SA-MAC protocol can be found in Section 3, the discrete Markov chain based numerical analysis is derived in Section 4. Complexity analysis of the SA-MAC protocol is carried out in Section 5. Experimental setup and numerical results are demonstrated in Section 6. Finally, the conclusion is presented in Section 7. In addition, Tables 1 and 2 present the list of abbreviations and symbols used in the paper, respectively.

**Table 2**  
List of symbols.

$A$	Area of ceiling
$C_\gamma$	Normalized collision probability of node $\gamma$
$e$	Number of state for Markov chain model
$E(\gamma)$	Normalized power consumed by node $\gamma$ in state $e$
$H_0^k$	DC channel gain threshold of a sub-carrier for $k$ request
$H_0^q$	DC channel gain of a sub-carrier for $q$ resource
$H_0^{k,q}$	Separation between DC channel gain of a sub-carrier and threshold for $k$ request from $q$ resources
$i_t$	Duration of idle time with geometric random variable
$k$	Number of request received from nodes
$K$	Number of nodes in back-off
$L_A$	Packet length
$m$	Generated packet number for node $\gamma$
$n$	Number of contending nodes in the network
$N$	Number of nodes
$N_C$	Normalized network collision probability
$N_D$	Normalized network delay
$N_E$	Normalized network energy consumption
$\eta_i$	Number of nodes in the PT for $i$ th superframe
$p(\gamma_i)$	Probability of node $\gamma$ to generate packets in BS
$p(\gamma_b)$	Probability of node $\gamma$ to receive the BC
$p(\gamma_{co})$	Probability of collision
$p_f$	Probability of AP failure
$p(\gamma_{rts})$	Probability of sending RTS
$p(\gamma_{cts})$	Probability of receiving CTS
$p(\gamma_i)$	Probability of back-off failure
$p(\gamma_s)$	Probability of transmitting successfully $r$ out of $m$ packets
$P_{CFP}$	Probability of successful transmission
$r$	Number of successfully transmitted packets
$PT_i$	PT in the $i$ th superframe
$R$	Maximum range of the LED array of AP
$S(\gamma), A(\gamma)$	Status of node $\gamma$ for 2D Markov chain model
$t_i$	Duration of $i$ th superframe
$W$	Window size for a constant back-off
$W_K$	The $K$ th node back-off state
$\pi_e$	Steady-state probability of node $\gamma$ being in state $e$
$\alpha$	Maximum round trip time between AP and nodes
$\beta$	BC duration
$\phi_i$	CAP duration in $t_i$
$\psi_i$	CFP duration in $t_i$
$\lambda$	Packet arrival rate
$\tau$	Stationary probability of transmitting a packet at a random time for node
$q$	Number of resources
$\delta_\gamma$	Delay of node $\gamma$
$\varepsilon_\gamma$	Normalized energy consumed by node $\gamma$

### 1.1. Related studies

An indoor aggregated WiFi-VLC wireless network that takes into account full-duplex communication is proposed in [5]. The authors in this study suggest the use of asymmetric VLC-RF system that utilizes RF for the uplink and VLC for the downlink channel. Moreover, the authors in [5] provide sufficient details about the network addressing problem for hybrid VLC-RF wireless networks. However, they did not describe the problem of MAC.

In order to improve energy efficiency in wireless networks, a hybrid VLC-RF system is proposed in [8]. The problem is modelled as NP-complete, and the results from the simulation are promising. In [6], the problem of network resource optimization for heterogeneous VLC-WiFi networks is investigated. The authors modelled the problem of resource optimization in VLC-RF wireless networks as a Lyapunov optimization, and the numerical results show the trade-off between delay and throughput. While targeting throughput and transmission probability, a parallel transmission MAC (PT-MAC) protocol for indoor hybrid VLC-RF wireless networks is suggested in [7]. The PT-MAC takes into consideration the CSMA/CA in its design and increases network throughput and transmission probability.

In [9], the delay analysis for unsaturated full-duplex VLC-RF wireless networks is suggested. The authors consider aggregated and non-aggregated scenarios in evaluating the delay of co-existing VLC-RF

wireless networks. Numerical results from their study show that aggregated scenario provides lower delay than the non-aggregated scenario. The authors in [10] designed and analysed the hybrid VLC–RF system wherein numerical results show that per node outage probability decreases in the hybrid VLC–RF networks. Moreover, the design and analysis of both hybrid and aggregated VLC–RF wireless networks presented in [11] show that the aggregated VLC–RF wireless network that considers each request RF for uplink and VLC for downlink provides high throughput and more reliable data transmission than hybrid VLC–RF network that considers each request either RF or VLC. In addition, the authors provide a detailed mechanism about network addressing in aggregated VLC–RF wireless networks.

A hybrid VLC–RF system comprised of duplex WiFi link and asymmetric duplex WiFi-VLC link is designed and implemented in [12]. The asymmetric link consists of a VLC downlink and a WiFi uplink. Network throughput of the aggregated system is measured and compared against a standalone WiFi system. Numerical results from this study reveal that the aggregated system outperforms the standalone WiFi system in terms of network throughput, utilization, and delay.

There are several research publications that address the quest for VLC-based MAC protocols such as [13–22]. However, they are restricted to half-duplex and hybrid VLC–RF wireless networks. Wang et al. in [23] present a full-duplex MAC protocol for VLC that allows concurrent sending and receiving data. They consider a star network topology in which visible light of different wavelength can be used for bidirectional transmissions. Existing research publications suggest different MAC protocols for hybrid VLC–RF wireless networks. The adaptive polling MAC protocol for aggregated infrared-VLC wireless networks is presented in [24] wherein the focus is minimizing network delay and increasing throughput. Unlike in [24], this study suggests the MAC protocol for aggregated VLC–RF wireless networks taking into consideration full-duplex communication aspect.

The major contributions of our study are listed as follows; (i) The SA-MAC protocol for aggregated VLC–RF networks, which exploits CSMA/CA and sub-carrier orthogonal techniques, are presented. The SA-MAC protocol has been extensively provided to demonstrate the main benefits of full duplex VLC–RF communication. Also, the performance of the proposed protocol is compared with existing protocols in terms of throughput, fairness, energy efficiency, and transmission probability. (ii) A dynamic superframe size algorithm, which depends on the number of nodes in an aggregated VLC–RF network, is introduced. (iii) A 2D Markov chain model-based analysis is conducted to obtain the numerical results of our protocol. It enables performance comparison between the simulation results and the numerical results. (iv) We adapt the DFK MTU algorithm [24] to our SA-MAC protocol for aggregated VLC–RF networks. (v) The NS3 network simulator is utilized for modelling and simulating the proposed SA-MAC protocol.

## 2. Network topology and problem statement

For simplicity, we consider an aggregated VLC–RF wireless network that contains a single access point (AP) and several nodes. The AP is located at the ceiling of the building while nodes are located at the ground of the building. The AP consists of a MAC control-unit (CU), LED for both illumination and transmitting signals, and NICs for VLC and RF. Nodes consist of photodiodes (PDs) for receiving signal from LED, CU, RF-NIC and VLC-NIC. Transmission from nodes to the AP (uplink channel) uses RF while transmission from the AP to nodes (downlink channel) uses VLC. Fig. 1 illustrates a simple indoor aggregated VLC–RF wireless network. Note that the addition of NIC in both AP and nodes introduces network addressing and MAC problems. Thus, the primary challenges in implementing aggregated VLC–RF wireless networks are network addressing and MAC.

In transmission control protocol, the connection is established by the client through an initiation of a three-way handshaking with the server. When the connection is established, the client generates a

synchronize message and encapsulates it in the internet protocol header prior to sending it by using the NIC. Following this, the client listens to the socket that contains transmission control protocol port number and internet protocol address used to generate and encapsulate the synchronize message. In this case, any reply packets received from the server with different NIC and different socket details are ignored. Network addressing in hybrid VLC–RF has been extensively studied in [11,12]. For simplicity and without loss of generality, in our study, we leverage the network addressing techniques suggested in [11].

Furthermore, in the RF domain, the carrier sense multiple access with collision avoidance (CSMA/CA) protocol is used to control access to a shared medium. There are two strategies of controlling access to a shared medium in VLC wireless networks such as orthogonal frequency division multiple access (OFDMA), and non-orthogonal multiple access [25]. Therefore, there is the need for designing the MAC protocol that takes into consideration the physical properties of the RF and VLC in aggregated VLC–RF wireless networks.

We suggest a polling based protocol wherein nodes request access to a shared medium in the uplink domain by using CSMA/CA. The downlink channel is shared by using sub-carrier orthogonality. Multiple nodes in a network can receive signals from the AP based on sub-carrier orthogonality. The challenge of using OFDMA in VLC is that, sub-carrier with low frequency provides high signal-to-noise ratio. Therefore, we provide a resource assignment algorithm that ensures that all nodes are treated fairly.

## 3. The self-adaptive medium access control (SA-MAC) protocol

The SA-MAC protocol for aggregated VLC–RF wireless networks involves three duration, viz., the beacon (BC) duration, the contention access period (CAP), and the contention-free period (CFP). In each duration, visible light AP and visible light nodes perform several activities. Below we narrate the superframe structure, activities of nodes and AP in our protocol. The mechanisms of BC, CAP, and CFP are described in this Section.

### 3.1. SA-MAC superframe structure

In the SA-MAC protocol, we consider a superframe that consists of BC, CAP, and CFP as shown in Fig. 2. In this protocol, the communication between node and AP can be provided by BC frame, request-to-send (RTS) frame, clear-to-send (CTS) frame, data transmission (DTF) frame, acknowledgement (ACK) frame.

---

#### Algorithm 1 Dynamic superframe size algorithm.

---

```

1: Input:  $i$ ,  $PT_{i-1}$ ,  $\eta_i$ ,  $t_i$ ,  $t_{i-1}$ ,  $\phi_{i-1}$ ,  $\psi_{i-1}$  and  $PT_i$ 
2: Initialization:  $\beta = 2\alpha$ ,
3: for each  $i$  do
4:   if  $PT_i = \emptyset$  then
5:      $\phi_i \leftarrow (\phi_{i-1})/2$ ,
6:      $\psi_i \leftarrow (\psi_{i-1})/2$ ,
7:      $t_i \leftarrow \beta + \phi_i + \psi_i$ 
8:   EndIf
9:   if  $PT_i \leq PT_{i-1}$  then
10:     $t_i \leftarrow t_i - |t_i - t_{i-1}|$ ,
11:     $\phi_i \leftarrow \eta_i * \alpha$ ,
12:     $\psi_i \leftarrow t_i - (\phi_i + \beta)$ 
13:   EndIf
14:   if  $PT_i > PT_{i-1}$  then
15:     $t_i \leftarrow t_i + |t_i - t_{i-1}|$ ,
16:     $\phi_i \leftarrow \eta_i * \alpha$ ,
17:     $\psi_i \leftarrow t_i - (\phi_i + \beta)$ 
18:   EndIf
19: EndFor

```

---

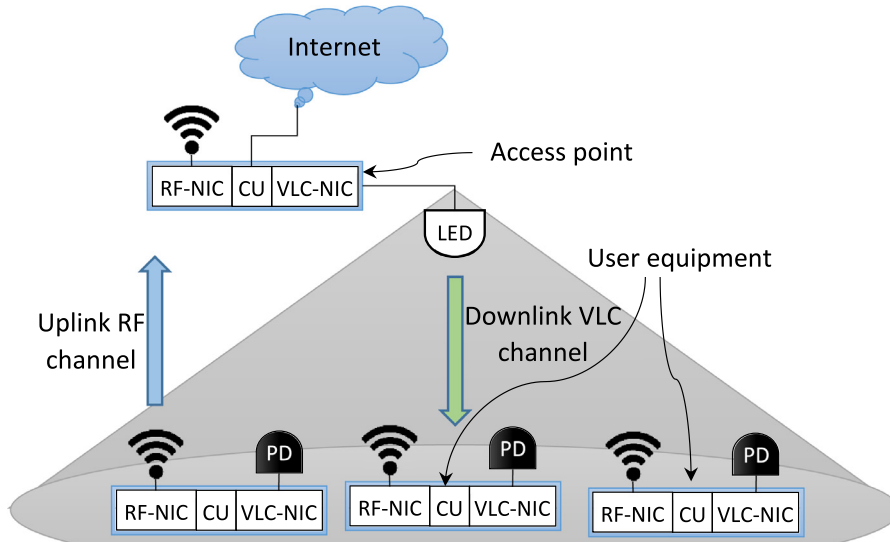


Fig. 1. Aggregated VLC-RF indoor wireless network.

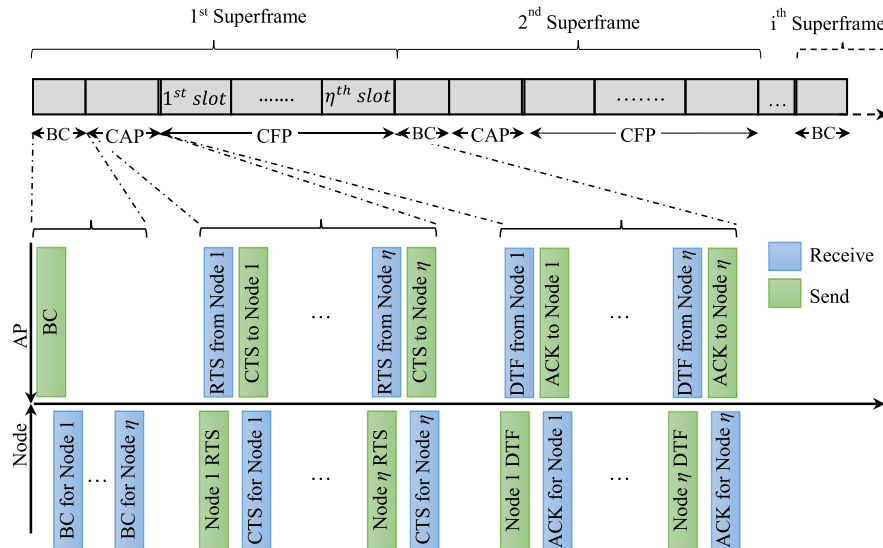


Fig. 2. Superframe structure and SA-MAC sequence diagram.

In the BC duration, the AP broadcasts the BC to all nodes. This is done by using the LED of the AP. The BC frame helps time synchronization between nodes and AP. During CAP, nodes request timeslot from the AP. The association phase involves sending the RTS message and receiving the CTS message from the AP. In the CFP there is no contention, a specific timeslot is assigned to each node. The size of each node's timeslot is determined by the AP depending on the request from nodes and the size of the CFP. In order to achieve optimal results, we introduce the dynamic superframe algorithm that approximates optimal superframe size. The dynamic superframe size is achieved by periodically adjusting the CAP and CFP depending on the number of nodes in the PT.

We consider three cases; (i) when the current PT contains no request, (ii) when the current PT contains fewer requests than the PT of the previous superframe, and (iii) when the current PT contains more requests than the PT of the previous superframe. In the first case, the current superframe size, considering the BC duration, is almost half of the previous superframe size. In the second case, the current superframe size is obtained by deducting the absolute difference between the previous and current superframe from the current superframe. In

the last case, the current superframe size is obtained by adding the absolute difference between the previous and current superframe to the current superframe. Algorithm 1 describes the mechanism of obtaining dynamic superframe size in our protocol. The size of each duration is also determined in this algorithm. In Algorithm 1,  $\eta_i$  denotes the number of nodes in the PT of  $i$ th superframe,  $\alpha$  corresponds to the maximum round trip time (RTT) between AP and nodes,  $t_i$  is the duration of  $i$ th superframe,  $PT_i$  is the PT in the  $i$ th superframe,  $\beta$  represents the BC duration,  $\phi_i$  is the CAP duration in  $t_i$ , and  $\psi_i$  is the CFP duration in  $t_i$ .

### 3.2. Access point flow

Fig. 3 shows the flowchart of the AP in the SA-MAC protocol for the aggregated VLC-RF wireless networks. APs and nodes run the SA-MAC protocol to communicate with each other. Initially, the AP broadcasts the BC frame to all nodes in the network. The BC frame contains the physical address of the AP, the superframe duration ( $t$ ), and the size of the CAP ( $\phi$ ). After broadcasting the BC frame, the AP sets its

timer to zero, then it delays for CAP receiving requests from nodes via RTS messages. In addition, the AP establishes the PT, in which all requests from the nodes via RTS messages are recorded, at the end of CAP. Then, the AP checks if there is any request received from nodes, i.e., PT is not empty. If the PT is empty, the AP starts the process again by broadcasting the BC frame, otherwise, it assigns resources to all requests. The AP performs a dynamic size determination by updating  $t_i$ ,  $\phi_i$ , and  $\psi_i$  duration for  $i$ th superframe. Following resource assignment, the AP sends CTS message to all nodes in the PT. After sending CTS messages to all nodes, the AP receives DTF from nodes and sends ACK frame within the CFP. At the end of the CFP, the AP begins a new superframe by sending another BC frame.

The mechanism of assigning resources at the AP is significant in the performance of the network, i.e., it can increase network delay. Therefore the mechanism of resource assignment employed in this study is presented in Algorithm 2. We devise a resource assignment algorithm that assigns resources ( $q$ ) to requests ( $k$ ) received from nodes fairly. Fairness is defined as taking into account MTU, time of request ( $i$ th superframe), and  $H_0^{k,q}$ , which is the separation between DC channel gain of a sub-carrier and defined threshold. This algorithm calculates this distance. Here,  $t_{k,q}$  is the time allocated to the  $q$ th resource allocated against the  $k$ th request. The timeslot is done by considering the requesting transmission size and the current MTU, which is the size of the largest data unit. Requests from nodes are recorded in a PT according to the order of arrival. Before resource assignment, requests are classified into three groups depending on the DC channel gain threshold of each request. Here, each group signs to one sub-carrier, i.e., R, G, and B since we consider trichromatic LED. The request is placed into a sub-carrier that has the shortest distance with respect to DC channel gain threshold. For each group, the assignment is done based on arrival rate, each request is assigned a timeslot in a corresponding sub-carrier. In aggregated VLC-RF network, obtaining DFK MTU [24,26] for each PT is shown in Algorithm 3. This algorithm provides the AP to adapt the size of the MTU depending on the current PT content.

#### Algorithm 2 Resource assignment algorithm

```

1: for each superframe do
2: Input: set of sub-carriers = {R,G,B} and PT.
3:   for corresponding CAP do
4:     for  $k \in PT$  do
5:       for  $q \in \{R, G, B\}$  do
6:          $H_0^{k,q} = H_0^q - H_0^k$ 
7:       EndFor
8:     EndFor
9:     while  $H_0^{k,q+1} \neq NULL$  do
10:      if  $H_0^{k,q} \leq H_0^{k,q+1}$  then
11:         $q \leftarrow k$ 
12:      Else
13:         $(q + 1) \leftarrow k$ 
14:      EndIf
15:    EndWhile
16:    for each  $q \in \{R, G, B\}$  do
17:      while request record in  $q \neq \emptyset$  do
18:        while CFP in  $q \neq 0$  do
19:           $t_{k,q} \leftarrow MTU$ 
20:           $k \leftarrow t_{k,q}$ 
21:          CFP in  $q = CFP$  in  $q - t_{k,q}$ 
22:        EndWhile
23:      EndWhile
24:    EndFor
25:  EndFor
26: EndFor
```

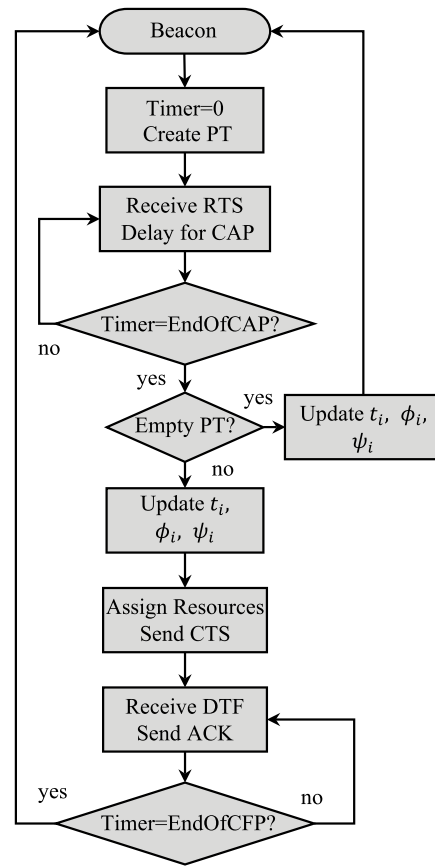


Fig. 3. The access point flowchart for the SA-MAC protocol.

#### 3.3. Network nodes flow

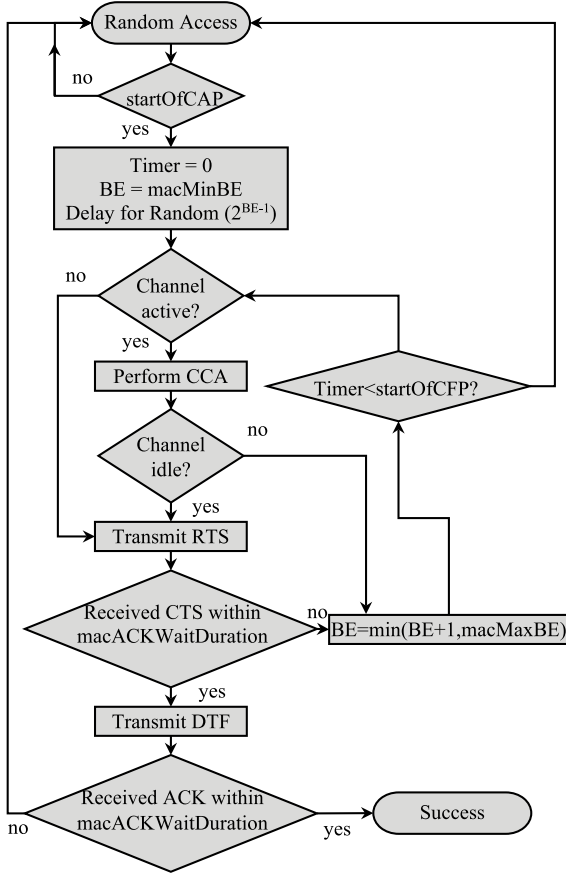
Initially, a node waits for the BC frame from the AP. Immediately after receiving the BC frame, a node sets the values of beacon exponents (BE), and timer. Unlike other CSMA-based protocols, in our protocol a node can start the back-off process depending on the probability of successful transmission. Thus, we minimize energy consumption by avoiding unnecessary channel sensing. If the probability of successful transmission is greater than zero, a node can start the back-off process, then it performs channel sensing. If the channel is not active, the RTS is sent to the AP. However, if the channel is active, then a node keeps performing the clear channel assessment (CCA) depending on the probability of successful transmission until the channel is detected idle. After sending RTS, a node waits for a CTS message from the AP within the maximum acceptable time. Failure to receive the CTS prompts a node to select another BE and checks if the CAP has elapsed. Carrier sense can be performed again if the CAP period has not elapsed, otherwise, a node waits for CAP of the next superframe in order to perform back-off process and channel sensing. If the CTS message arrives within the acceptable time, then a node sends data to the AP and waits for ACK frame. Un-acknowledgement of transmitted data implies unsuccessful transmission, therefore, a node randomly selects another BE and begins channel sensing again in the CAP of the next superframe. Thus, the process of association is restricted to the CAP, therefore, RTS messages arriving at the AP during CFP are ignored. Fig. 4 illustrates the node flowchart in the aggregated VLC-RF wireless networks. Here, macMinBE and macMaxBE are minimum and maximum back-off exponents, respectively. The value of macAckWaitDuration is the maximum waiting time for receiving frame, i.e., ACK and CTS. The startOfCAP and startOfCFP values are the starting time of CAP and CFP frames.

**Algorithm 3** DFK MTU algorithm for the VLC-RF network

```

1: Input:  $i$  and  $PT_i$ ,
2: for each  $i$  do
3:    $MTU_i = \text{Mean of the } PT_i$ ,
4:   while  $PT_i \neq \emptyset$  do
5:     for each node  $\gamma : \{\gamma = 1, \dots, n\} \in PT_i$  do
6:       if node  $\gamma$  buffer  $\geq MTU_i$  then
7:          $MTU_i$  is the MTU for node  $\gamma$ ,
8:       EndIf
9:       if node  $\gamma$  buffer  $< MTU_i$  then
10:        The buffer size of  $\gamma$  is the MTU for node  $\gamma$ ,
11:      EndIf
12:    EndFor
13:  EndWhile
14: EndFor

```

**Fig. 4.** The node flowchart in SA-MAC protocol.**4. Performance analysis**

We present the 2D Markov chain model wherein states of node  $\gamma$  are represented as  $(S(\gamma), A(\gamma))$ . In this context,  $S(\gamma)$  represent the status of node  $\gamma$ , i.e., BC state  $S(\gamma) = S$ , CAP state  $S(\gamma) = 2S$ , and CFP state  $S(\gamma) = 3S$ . Moreover, in each state,  $A(\gamma)$  takes different interpretations as follows:

- When node  $\gamma$  is in state  $S$ , then  $A(\gamma)$  is 0 if no packets arrive at node  $\gamma$  and 1 if packets arrive at node  $\gamma$ . Then  $A(\gamma)$  is 2 if the BC frame is not received and 3 if the BC frame is received.
- The states from  $(2S, 0)$  to  $(2S, 1)$  represent the back-off states. When node  $\gamma$  is in state  $2S$ , then  $A(\gamma)$  is 0 if back-off process is

**Table 3**  
2D Markov chain model states definition.

State name	$S(\gamma)$	$A(\gamma)$	Explanation
BC	S	0	No packets are generated at node $\gamma$
		1	Packets are generated at node $\gamma$
		2	BC frame not is received at node $\gamma$
		3	BC frame is received at node $\gamma$
CAP	2S	0	Back-off is not initiated at node $\gamma$
		1	End of back-off process
		2	RTS is transmitted from node $\gamma$
		3	CTS is received at node $\gamma$
		4	CTS is not received at node $\gamma$
CFP	3S	0	No packets are transmitted
		1	If all packets are transmitted successfully
		2	If some packets are not transmitted

not initiated, between 1 – 2 if back-off is initiated, 2 if RTS is transmitted, 3 if CTS is received and 4 if CTS is not received.

- When node  $\gamma$  is in state  $3S$ , then  $A(\gamma)$  is defined as 1 if all packets are transmitted and acknowledged successfully, otherwise it is 2. If no packets are transmitted then,  $A(\gamma)$  is 0. Where  $L_A$  is the length of a packet.

In Table 3 we present a summary of the Markov chain model for our protocol. Moreover, Fig. 5 shows the Markov chain model of the SA-MAC protocol for aggregated VLC-RF wireless networks. Here, the state transitions among superframes are depicted with different lines. Accordingly, while the current superframe state transitions are shown with a straight line, a dashed line is used to switch from the current superframe to next superframe transition states. Bianchi [27] and Shams [28] Markov-based models are considered for back-off, transmission and ACK states in this model. If  $S(\gamma) \in 0, \dots, K$ , the station is in back-off state,  $A(\gamma)$  can get any value from set of  $0, \dots, W_K - 1$ , depending back-off counter. We study the behaviour of a single node by using the Markov chain model that consists of three states defined above.

**4.1. Defining transition probabilities**

The process of packet arrival is generally modelled as Poisson distribution, therefore, we assume that same distribution can be adopted for the probability of the node to generate packets in BC state. Thus, the probability of node  $\gamma$  to generate packets in BC state is defined as:

$$p(\gamma_i) = \frac{(\lambda i_t)^m e^{-\lambda i_t}}{m!}, \quad (1)$$

where  $m$  is the number of packets generated,  $i_t$  is the duration of idle time with geometric random variable and  $\lambda$  is the packet arrival rate. Moreover, when the AP broadcasts the BC frame, node  $\gamma$  receives the BC frame with some probabilities  $p(\gamma_b)$ . Note that  $p(\gamma_b)$  depends on the position of the node. Otherwise, it will not detect any signal from the AP [29]. We therefore, define  $p(\gamma_b)$  as follows:

$$p(\gamma_b) = 1 - \left(1 - \frac{\pi R^2}{A}(1 - p_f)\right)^N, \quad (2)$$

where  $N$  is the number of nodes,  $R$  is the maximum range of the LED array of AP,  $A$  is the area of the ceiling, and  $p_f$  is the probability of AP failure. Moreover,  $p(\gamma_{rts})$  is the probability of sending RTS and  $p(\gamma_{cts})$  is the probability of receiving CTS, i.e. a node is in the state  $(2S, 3)$ . The collision probability,  $p(\gamma_c)$ , is the probability of receiving CTS given sending RTS, can be expressed as:

$$p(\gamma_c) = p(\gamma_{cts} | \gamma_{rts}). \quad (3)$$

The probability of sending RTS and receiving CTS depends on the probability of receiving a BC frame, and the probability of successful

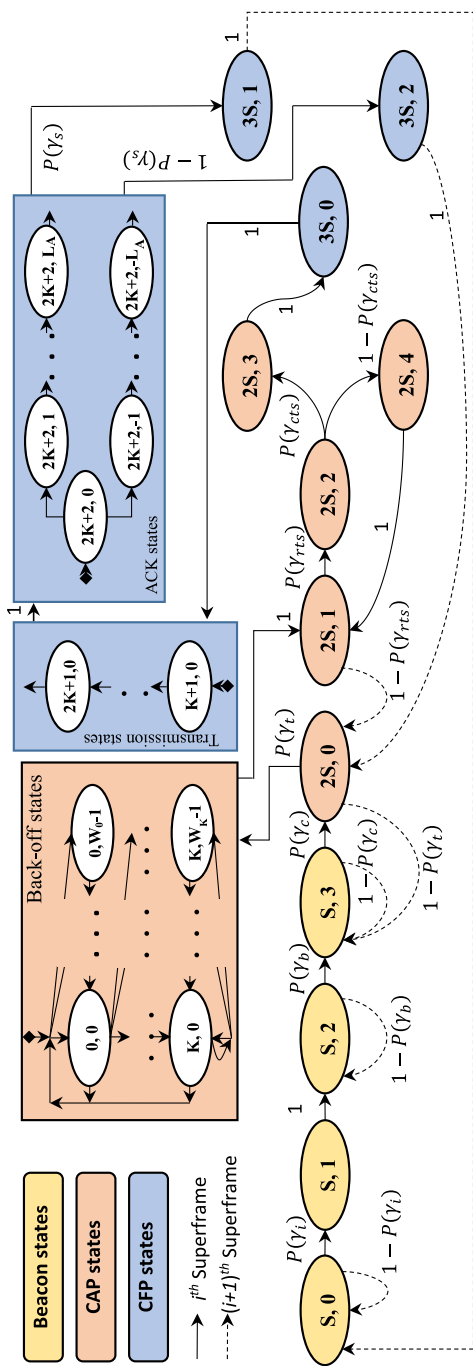


**Fig. 5.** The Markov chain model for SA-MAC protocol.

transmission of RTS. The probability of successful transmission of RTS is given by the probability that exactly one station transmits on the channel, conditioned on the fact that at least one station transmits proved by authors of [27] for a constant back-off window.

$$p(\gamma_{rts}) = \frac{n\tau(1-\tau)^{n-1}}{1-(1-\tau)^n}, \quad (4)$$

where  $n$  is the number of contending nodes in a network,  $\tau$  is the stationary probability that a node transmits a packet at a random time. For a constant back-off size, and window size  $W$ ,  $\tau$  is defined as follows [27]:

$$\tau = \frac{2}{W+1}. \quad (5)$$

Note that  $p(\gamma_t)$  in Fig. 5 is equal to  $p(\gamma_{rls})$  and the downlink channel uses VLC, thus  $p(\gamma_{cls})$  can be determined like  $p(\gamma_b)$ ,

$$p(\gamma_{cts}) = p(\gamma_b). \quad (6)$$

In CFP, the probability of successful transmission is  $P_{CFP}$  and  $1 - P_{CFP}$  is the probability of transmission failure. If node  $\gamma$  generates  $m$  packets, the probability of transmitting successfully  $r$  out of  $m$  packets is given as:

$$p(\gamma_s) = \binom{m}{r} \cdot P_{CFP}^r (1 - P_{CFP})^{m-r}. \quad (7)$$

#### 4.2. Throughput analysis

We assume that a node generates  $n$  packets of equal length  $L$ . A node can successfully send packets it reaches the final state, i.e.,  $\pi_{(3S,1)} > 0$ . Thus, we can establish the throughput of a node if we determine the probability of being in the final state. Let  $\pi_e|e = \{0, \dots, 11\}$  be the steady-state probability of node  $\gamma$  being in state  $e$ , i.e.,  $\pi_e = P(\gamma_e)$ , where  $\{\pi_0 = (S, 0), \pi_1 = (S, 1), \pi_2 = (S, 2), \pi_3 = (S, 3), \pi_4 = (2S, 0), \pi_5 = (2S, 1), \pi_6 = (2S, 2), \pi_7 = (2S, 4), \pi_8 = (2S, 3), \pi_9 = (3S, 0), \pi_{10} = (3S, 2), \pi_{11} = (3S, 1)\}$ . We define the equations for steady-state distribution and obtain the steady-state probabilities as follows:

$$\pi_0 p(\gamma_i) = \pi_0(1 - p(\gamma_i)) + \pi_{11} \quad (8a)$$

$$\pi_1 = \pi_0 p(\gamma_i) \quad (8b)$$

$$\pi_2 p(\gamma_b) + \pi_2(1 - p(\gamma_b)) = \pi_1 \quad (8c)$$

$$\pi_3 p(\gamma_c) + \pi_3(1 - p(\gamma_c)) = \pi_2 p(\gamma_b) \quad (8d)$$

$$\pi_4 p(\gamma_t) + \pi_4 (1 - p(\gamma_t)) = \pi_3 p(\gamma_c) \quad (8e)$$

$$\pi_5 p(\gamma_{rts}) + \pi_5(1 - p(\gamma_{rts})) = \pi_4 p(\gamma_t) + \pi_7 \quad (8f)$$

$$\pi_6 p(\gamma_{cts}) + \pi_6(1 - p(\gamma_{cts})) = \pi_5 p(\gamma_{rts}) \quad (8g)$$

$$\pi_7 = \pi_6(1 - p(\gamma_{cts})) \quad (8h)$$

$$\pi_8 = \pi_6 p(\gamma_{cts}) \quad (8i)$$

$$\pi_9 p(\gamma_s) + \pi_9(1 - p(\gamma_s)) = \pi_8 \quad (8j)$$

$$\pi_{10} = \pi_9(1 - p(\gamma_s)) \quad (8k)$$

$$\pi_{11} = \pi_9 p(\gamma_s) \quad (8l)$$

Note that in steady-state the probability distribution for all states must sum to 1, i.e.

$$\sum_{e=(S,0)}^{3S,1} \pi_e = 1 \quad (9)$$

After solving these linear equations, we get the following values of steady-state probabilities:

$$\pi_0 = [p(\gamma_i) - (1 - p(\gamma_i))]^{-1} \quad (10)$$

$$\pi_1 = \frac{p(\gamma_i)}{p(\gamma_i) - (1 - p(\gamma_i))} \quad (11)$$

$$\pi_2 = \left[ p(\gamma_b) + (1 - p(\gamma_i)) \right]^{-1} \quad (12)$$

$$\pi_3 = \frac{p(\gamma_b)}{\left[ p(\gamma_c) + (1 - p(\gamma_c)) \right] \left[ p(\gamma_d) + (1 - p(\gamma_d)) \right]} \quad (13)$$

$$\pi_4 = \left[ \begin{array}{c} p(\gamma_b) \\ \hline [p(\gamma_c) + (1 - p(\gamma_c))] [p(\gamma_b) + (1 - p(\gamma_i))] \end{array} \right] \\ \left[ \begin{array}{c} p(\gamma_t) \\ \hline [p(\gamma_t) + (1 - p(\gamma_t))] \end{array} \right] \quad (14)$$

$$\pi_5 = \left[ \begin{array}{c} p(\gamma_b) \\ \hline [p(\gamma_c) + (1 - p(\gamma_c))] [p(\gamma_b) + (1 - p(\gamma_i))] \end{array} \right] \\ \left[ \begin{array}{c} p(\gamma_t) \\ \hline [p(\gamma_t) + (1 - p(\gamma_t))] \end{array} \right] \left[ \begin{array}{c} (p(\gamma_t)) \\ \hline [p(\gamma_{rts}) + (1 - p(\gamma_{rts}))] \end{array} \right] \quad (15)$$

$$\pi_6 = \left[ \begin{array}{c} p(\gamma_b) \\ \hline [p(\gamma_c) + (1 - p(\gamma_c))] [p(\gamma_b) + (1 - p(\gamma_i))] \end{array} \right] \\ \left[ \begin{array}{c} p(\gamma_t) \\ \hline [p(\gamma_t) + (1 - p(\gamma_t))] \end{array} \right] \left[ \begin{array}{c} (p(\gamma_t)) \\ \hline [p(\gamma_{rts}) + (1 - p(\gamma_{rts}))] \end{array} \right] \\ \left[ \begin{array}{c} p(\gamma_{rts}) \\ \hline [p(\gamma_{cts}) + (1 - p(\gamma_{cts}))] \end{array} \right] \quad (16)$$

$$\pi_7 = [(1 - p(\gamma_{cts}))] \left[ \begin{array}{c} p(\gamma_{rts}) \\ \hline [p(\gamma_{cts}) + (1 - p(\gamma_{cts}))] \end{array} \right] \\ \left[ \begin{array}{c} p(\gamma_b) \\ \hline [p(\gamma_c) + (1 - p(\gamma_c))] [p(\gamma_b) + (1 - p(\gamma_i))] \end{array} \right] \\ \left[ \begin{array}{c} p(\gamma_t) \\ \hline [p(\gamma_t) + (1 - p(\gamma_t))] \end{array} \right] \left[ \begin{array}{c} (p(\gamma_t)) \\ \hline [p(\gamma_{rts}) + (1 - p(\gamma_{rts}))] \end{array} \right] \quad (17)$$

$$\pi_8 = [p(\gamma_{cts})] \left[ \begin{array}{c} p(\gamma_{rts}) \\ \hline [p(\gamma_{cts}) + (1 - p(\gamma_{cts}))] \end{array} \right] \\ \left[ \begin{array}{c} p(\gamma_b) \\ \hline [p(\gamma_c) + (1 - p(\gamma_c))] [p(\gamma_b) + (1 - p(\gamma_i))] \end{array} \right] \\ \left[ \begin{array}{c} p(\gamma_t) \\ \hline [p(\gamma_t) + (1 - p(\gamma_t))] \end{array} \right] \left[ \begin{array}{c} (p(\gamma_t)) \\ \hline [p(\gamma_{rts}) + (1 - p(\gamma_{rts}))] \end{array} \right] \quad (18)$$

$$\pi_9 = [p(\gamma_{cts})] \left[ \begin{array}{c} p(\gamma_{rts}) \\ \hline [p(\gamma_{cts}) + (1 - p(\gamma_{cts}))] \end{array} \right] \left[ \begin{array}{c} p(\gamma_t) \\ \hline [p(\gamma_t) + (1 - p(\gamma_t))] \end{array} \right] \\ \left[ \begin{array}{c} p(\gamma_b) \\ \hline [p(\gamma_c) + (1 - p(\gamma_c))] [p(\gamma_b) + (1 - p(\gamma_i))] \end{array} \right] \\ \left[ \begin{array}{c} (p(\gamma_t)) \\ \hline [p(\gamma_{rts}) + (1 - p(\gamma_{rts}))] \end{array} \right] [p(\gamma_s) + (1 - p(\gamma_s))]^{-1} \quad (19)$$

$$\pi_{10} = [(1 - p(\gamma_s))] [p(\gamma_s) + (1 - p(\gamma_s))]^{-1} \\ \left[ \begin{array}{c} p(\gamma_{cts})p(\gamma_{rts}) \\ \hline [p(\gamma_{cts}) + (1 - p(\gamma_{cts}))] \end{array} \right] \left[ \begin{array}{c} p(\gamma_t) \\ \hline [p(\gamma_t) + (1 - p(\gamma_t))] \end{array} \right] \\ \left[ \begin{array}{c} p(\gamma_b) \\ \hline [p(\gamma_c) + (1 - p(\gamma_c))] [p(\gamma_b) + (1 - p(\gamma_i))] \end{array} \right] \\ \left[ \begin{array}{c} (p(\gamma_t)) \\ \hline [p(\gamma_{rts}) + (1 - p(\gamma_{rts}))] \end{array} \right] \quad (20)$$

$$\pi_{11} = [p(\gamma_s)p(\gamma_{cts})] \left[ \begin{array}{c} p(\gamma_b) \\ \hline [p(\gamma_c) + (1 - p(\gamma_c))] [p(\gamma_b) + (1 - p(\gamma_i))] \end{array} \right] \\ \left[ \begin{array}{c} p(\gamma_{rts}) \\ \hline [p(\gamma_{cts}) + (1 - p(\gamma_{cts}))] \end{array} \right] \left[ \begin{array}{c} p(\gamma_t) \\ \hline [p(\gamma_t) + (1 - p(\gamma_t))] \end{array} \right] \\ \left[ \begin{array}{c} (p(\gamma_t)) \\ \hline [p(\gamma_{rts}) + (1 - p(\gamma_{rts}))] \end{array} \right] [p(\gamma_s) + (1 - p(\gamma_s))]^{-1} \quad (21)$$

From this condition, the probability distribution for each state can be calculated. We calculate the throughput of a node as the probability of being in the final state i.e.,  $P(\gamma_e) = (3S, 1)$ , therefore, per node throughput is calculated as in Eq. (21).

#### 4.3. Network delay

Let  $\delta_\gamma$  be the delay of node  $\gamma$  and  $N_D$  be the network delay. From the Markov chain model, the delay of a node is the probability of moving from the initial state to the CFP. Mathematically, we represent this as follows:

$$\delta_\gamma = \bigcup_{e=(S,0)}^{(2S,3)} p(\gamma_{e+1} | \gamma_e). \quad (22)$$

Similarly, the expression above gives a delay of a single node. The network delay can be written as

$$N_D = \left( \sum_{\gamma=1}^N \bigcup_{e=(S,0)}^{(2S,3)} p(\gamma_{e+1} | \gamma_e) \right) N^{-1}. \quad (23)$$

#### 4.4. Power consumption

Let  $E(\gamma)$  denotes the normalized power consumed by node  $\gamma$  in state  $e$  and  $N_E$  be the normalized network energy consumption. The energy used by a node in each state depends on whether a node is idle, receiving, or transmitting. We minimize energy consumption in CAP by allowing the node to begin the back-off process depending on the successful data transfer probability. This is contrary to the CSMA protocol in which a node randomly initiates back-off process thereby, causing unnecessary energy consumption. For each transmission, the normalized energy consumed by node  $\gamma$  is denoted by  $\varepsilon_\gamma$  and is mathematically written as follows:

$$\varepsilon_\gamma = \bigcup_{e=(S,0)}^{(3S,1)} p(\gamma_{e+1} | \gamma_e) E(\gamma_{e+1}). \quad (24)$$

Extending the expression above yields the following network energy consuming equation,

$$N_E = \left( \sum_{\gamma=1}^N \bigcup_{e=(S,0)}^{(3S,1)} p(\gamma_{e+1} | \gamma_e) E(\gamma_{e+1}) \right) N^{-1}. \quad (25)$$

#### 4.5. Collision

Collision can occur in the uplink channel because of simultaneous transmission during CAP. Thus, a node encounters collision if it is in CAP and at least one of the remaining  $n - 1$  nodes transmit simultaneously. Let  $p(\gamma_c)$  denote the probability of collision that is defined as follows [27,30],

$$p(\gamma_c) = 1 - (1 - \tau)^{n-1}. \quad (26)$$

Therefore, the normalized collision of node  $\gamma$  denoted as  $C_\gamma$  can be expressed as a function of probability of being in CAP state and  $p(\gamma_c)$ ,

$$C_\gamma = \left( \bigcup_{e=(S,0)}^{(2S,2)} p(\gamma_{e+1} | \gamma_e) \right) (1 - (1 - \tau)^{n-1}). \quad (27)$$

We extend this expression to achieve the normalized network collision for  $N$  number of nodes as follows:

$$N_C = \left( \sum_{\gamma=1}^N \left( \bigcup_{e=(S,0)}^{(2S,2)} p(\gamma_{e+1} | \gamma_e) \right) (1 - (1 - \tau)^{n-1}) \right) N^{-1}. \quad (28)$$

#### 5. Complexity analysis of the SA-MAC protocol

The complexity analysis provides an approximate order number for the operations or steps to arrange and configure the duration and resource in each superframe in a VLC-RF aggregated network, as well as to guarantee the packet transmission requirements for both AP and nodes. To simplify the complexity analysis of the SA-MAC protocol, Fig. 6 shows the analysis for the dynamic superframe size algorithm and the resource assignment algorithm. The operations underlining the SA-MAC protocol scheme do not involve matrix–vector multiplication and

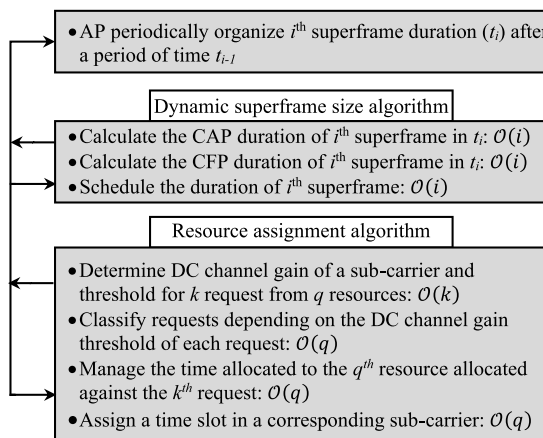


**Fig. 6.** The complexity analysis of the SA-MAC protocol.

matrix inversion. Therefore, the realization complexity of the proposed SA-MAC protocol is considered very low, as explained in Fig. 6. The complexity of the dynamic superframe size algorithm in SA-MAC, AP requires some operations of order  $\mathcal{O}(i)$ , where  $i$  denotes the number of the superframe. The same number of operations is required to calculate and schedule CFP duration and superframe duration, respectively. It has approximately the complexity of order  $\mathcal{O}(i)$ . However, the resource assignment algorithm has the complexity of order  $\mathcal{O}(kq)$ , where  $k$  denotes the number of requests received from nodes in the corresponding CAP duration. The AP organizes each superframe time regarding the reconfiguration of the CAP, CFP, and BC duration of the  $i^{\text{th}}$  superframe. It also manages resource allocation to request and their respective number of resources to guarantee their target downlink and uplink throughput, as shown in Fig. 6. Thus, the complexity of the proposed SA-MAC protocol for a VLC-RF aggregated network is approximate of order  $\mathcal{O}(ikq)$ . Several scalar operations of order  $\mathcal{O}(1)$  is also considered in this analysis.

## 6. Experimental setup and numerical results

We evaluate the performance of our protocol by taking into consideration network delay, throughput, collision, and energy consumption. We consider different sizes of a number of nodes for each performance metric.

In order to evaluate the performance of SA-MAC protocol, we simulate our protocol in the NS3 network simulator. The simulations are conducted in an IEEE 802.15.7 VLC MAC/PHY environment for VLC channels and IEEE 802.11n RF MAC/PHY for RF channels, and the results are discussed below. NS3 source codes can be found in [31]. For each performance metric, we compare simulation results with Markov chain model. We also compare our results with existing MAC protocols such as carrier sense multiple access with collision detection hidden node avoidance (CSMA/CD-HA) presented in, [32] and the dynamic contention window-based successive transmission (DCW-ST) suggested in [13]. BC frame length is chosen 0.5 slot as in [1], CAP and CFP periods are determined by Algorithm 1 with variable slot. VLC and RF subchannel bandwidths are chosen equally. The results presented in our study are obtained based on the detailed parameters in Table 4. For each performance metric, we run the simulation 50 times and the results presented are average.

### 6.1. Throughput

Network throughput is one of the performance metrics that we take into consideration in evaluating the benefits of our study. Throughput is the number of packets transmitted successfully divided by the total

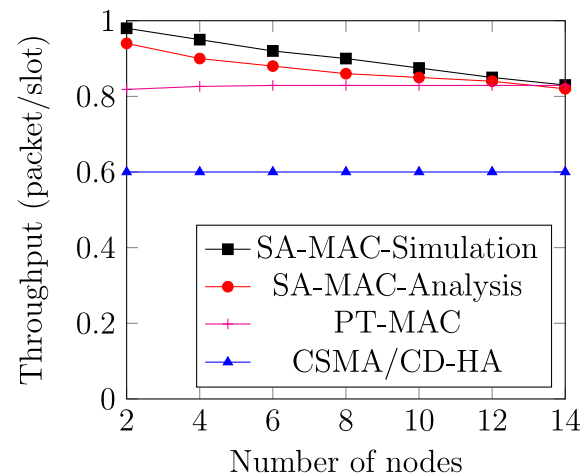


**Fig. 7.** Number of nodes versus normalized network throughput (in unit packet/slot).

**Table 4**  
Simulation parameters.

Description	Setting
Room size (Width × Length × Height)	4 m × 4 m × 2.5 m
Vertical separation	2.5 m
Field of view of the receiver	60°
Angle of the transmitter	30°
Optical concentrator refractive index	1.5
Photodetector area	1 [cm <sup>2</sup> ]
PD responsivity	0.6 A/W
VLC data rate per node	80 Mbps
RF Data rate per node	150 Mbps
Packet size ( $L_A$ )	1024 Bytes
Window size (W)	32
Mean packet arrival rate ( $\lambda$ )	5
Number of nodes ( $N$ )	2-14
aBaseSlotDuration [1]	60 slot
aBaseSuperframeDuration [1]	960 slot
aNumSuperframeSlots [1]	16 slot
macMaxBE and macMinBE [1]	5 and 3
VLC and RF subchannel bandwidths	20 MHz and 20 MHz

number of packets transmitted in each superframe. Fig. 7 presents the results considering networks size against normalized throughput. We compare results from SA-MAC simulation, Markov chain model, the PT-MAC and the CSMA/CD-HA protocol. Results in Fig. 7 suggest that throughput decreases when the number of nodes increases for both simulation and the Markov chain model. This is prompted by an increase in collision in the CAP state when the number of nodes increases. There is a slight difference between simulation and Markov chain model results at low number of nodes, however, the results converge when the number of nodes increases. Our simulation and Markov chain model results outperform the PT-MAC and the CSMA/CD-HA protocol in terms of throughput. Fig. 7 shows that the SA-MAC protocol achieves a better throughput performance than PT-MAC throughput below 14 nodes. For a number of nodes, SA-MAC and PT-MAC almost show the same throughput performance of about 0.82 packets/slot.

### 6.2. Network delay

We evaluate the performance of the SA-MAC protocol for aggregated VLC-RF wireless networks by considering network delay for both Markov chain model and simulation.

Numerical results in Fig. 8 suggest that simulation results show more delay compared to Markov chain model results, especially when the number of nodes is small. However, the difference in this case is not significant. Moreover, network delay is an increasing function of the number of nodes for both simulation and the Markov chain model. This

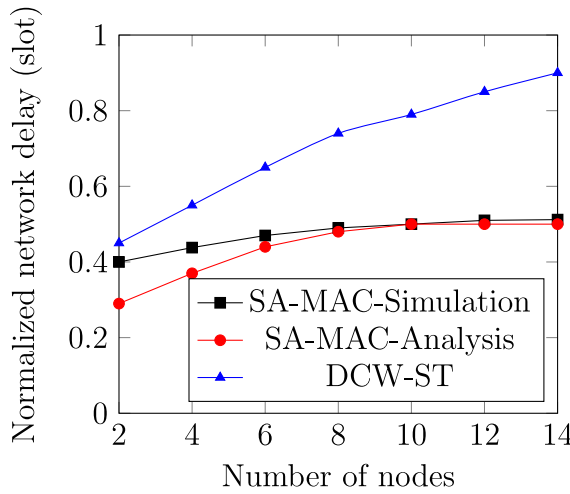


Fig. 8. Number of nodes versus delay (in time slot unit).

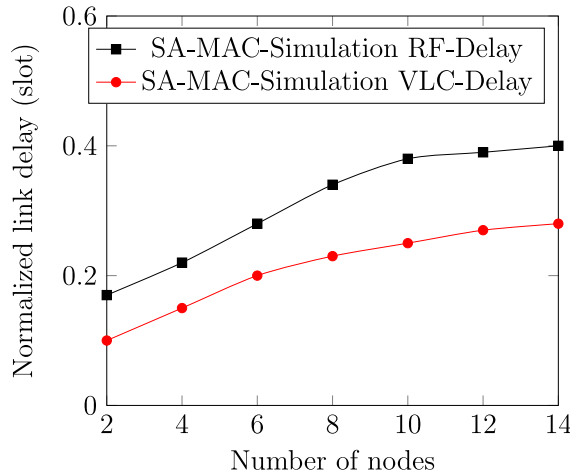


Fig. 9. Number of nodes versus link delay (in time slot unit).

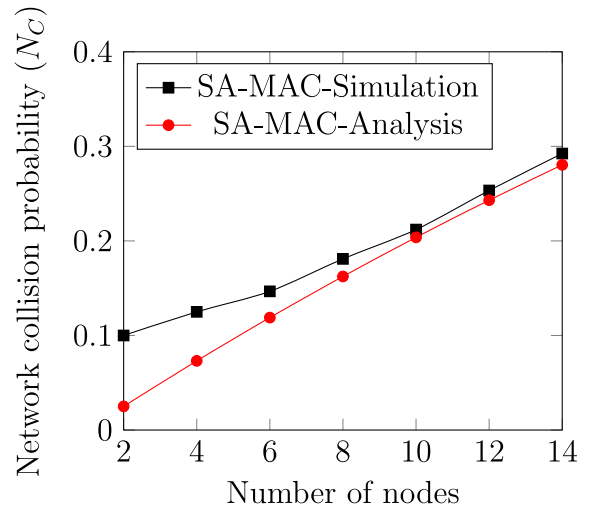


Fig. 10. Collision probability of different number of users.

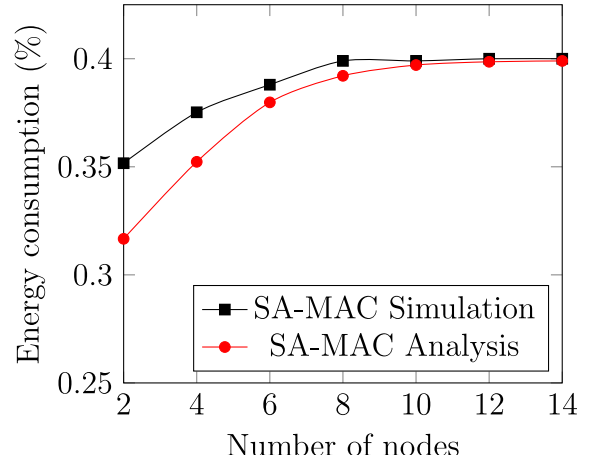


Fig. 11. Number of nodes versus energy consumption (in unit transmission power).

is because when the number of nodes is large, there is more competition for limited resources available at the AP, viz.,  $p(\gamma_{rt})$  decreases as suggested in Eq. (4). Fig. 8 also presents a comparison of our results against the results obtained in the DCW-ST protocol. In this case the SA-MAC protocol outperforms the DCW-ST in terms of networks delay especially when the number of nodes increases. Furthermore, we demonstrate the impact of RF and VLC channels in network delay in Fig. 9. Results from simulations show that RF-channels contribute more delay than the VLC-channel. This is due to the fact that RF-channel is used in CAP where there is contention. Moreover, the propagation speed of RF is lower than that of VLC. Note that, in Markov chain model, the behaviour of a system can be analysed based on transition and states probability. Therefore, it is not ideal to obtain delay contributed by individual links, i.e., VLC and RF links. Accordingly, in Fig. 9, we show results from the simulation only.

### 6.3. Collision

We describe the performance of our protocol by comparing probability of collision in the SA-MAC simulation and Markov chain model, and the results are presented in Fig. 10. In this context, collision probability refers to unsuccessful packet transmission. The results in this case suggest that collision increases when the number of nodes increases for both simulation and Markov chain model. For example, network collision increases from 0.1 when the number of nodes is 2

to 0.29 when the number of nodes is 14 for SA-MAC and from 0.025 when the number of nodes is 2 to 0.28 when the number of nodes is 14 for the Markov chain model results. Simulation results yield more collision than the Markov chain model results at when the number of nodes is small. However, difference between simulation results and Markov chain model is negligible, especially when the number of nodes increases.

### 6.4. Energy consumption

In Fig. 11, we present our results considering the rate of energy consumption. Similarly, we compare results from SA-MAC simulation with results from the Markov chain model. For simplicity, we assume that the distribution of energy consumption for the Markov chain model is 0.1, 0.4, and 0.5 in BC, CAP, and CFP states respectively. In this case, normalized energy consumption increases when the number of nodes increases for both the SA-MAC simulation and Markov chain model results, and it converges when the number of nodes is high, i.e. > 8. At a low number of nodes normalized energy consumption is low because the probability of collision is low, hence, small amount of energy is used during the association phase. Collision increases when the number of nodes increases as suggested by Eq. (25). However, at steady-state, the rate of collision remains constant.

## 7. Conclusion

The existing internet demand is overwhelming to the RF-based wireless networks. VLC can address the ever-increasing internet demand considering the huge bandwidth available in the visible light spectrum. Nevertheless, VLC standalone system cannot provide full-duplex communication because of several limitations such as network addressing, MAC, interference, and energy consumption of LEDs. The co-existence of RF and VLC systems can be used to achieve full-duplex communication in indoor wireless networks. In this study, we proposed the aggregate VLC–RF wireless network MAC protocol named SA-MAC protocol. We demonstrated the Markov chain model that shows the behaviour of a node in our protocol. The simulation of our protocol is done in the NS3 discrete event network simulator. In order to validate our study, the results from simulations and Markov chain model are compared for each performance metric. Furthermore, we showed the potential benefits of our study, by comparing our results against existing MAC protocols such as DCW-ST and CSMA/CD-HA. Numerical results from our study suggest that SA-MAC protocol outperforms existing MAC protocols for aggregated VLC–RF wireless networks. Note that, the SA-MAC protocol focuses on aggregated VLC–RF wireless networks. Designing MAC protocol for non-hybrid RF devices is beyond the scope of this study.

## Declaration of competing interest

The authors declare that they have no known competing financial interests or personal relationships that could have appeared to influence the work reported in this paper.

## References

- [1] IEEE Standard for local and metropolitan area networks—part 15.7: Short-range optical wireless communications, 2019, pp. 1–407, IEEE Std 802.15.7-2018 (Revision of IEEE Std 802.15.7-2011).
- [2] H. Haas, L. Yin, Y. Wang, C. Chen, What is LiFi?, *J. Lightwave Technol.* 34 (6) (2016) 1533–1544.
- [3] M. Ayyash, H. Elgala, A. Kheishah, V. Jungnickel, T. Little, S. Shao, M. Rahaim, D. Schulz, J. Hilt, R. Freund, Coexistence of WiFi and LiFi toward 5G: concepts, opportunities, and challenges, *IEEE Commun. Mag.* 54 (2) (2016) 64–71.
- [4] W. Abdallah, D. Krichen, N. Boudriga, An optical backhaul solution for LiFi-based access networks, *Opt. Commun.* 454 (2020) 124473.
- [5] S. Shao, A. Kheishah, M.B. Rahaim, H. Elgala, M. Ayyash, T.D.C. Little, J. Wu, An indoor hybrid WiFi-VLC internet access system, in: 2014 IEEE 11th International Conference on Mobile Ad Hoc and Sensor Systems, October 2014, Philadelphia, PA, USA, pp. 569–574.
- [6] W. Wu, F. Zhou, Q. Yang, Adaptive network resource optimization for heterogeneous VLC/RF wireless networks, *IEEE Trans. Commun.* 66 (11) (2018) 5568–5581.
- [7] W. Guo, Q. Li, H. Yu, J. Liu, A parallel transmission MAC protocol in hybrid VLC-RF network, *J. Commun.* 10 (2015) 80–85.
- [8] A. Kheishah, S. Shao, A. Gharaibeh, M. Ayyash, H. Elgala, N. Ansari, A hybrid RF-VLC system for energy efficient wireless access, *IEEE Trans. Green Commun. Netw.* 2 (4) (2018) 932–944.
- [9] S. Shao, A. Kheishah, Delay analysis of unsaturated heterogeneous omnidirectional-directional small cell wireless networks: The case of RF-VLC coexistence, *IEEE Trans. Wireless Commun.* 15 (12) (2016) 8406–8421.
- [10] D.A. Basnayaka, H. Haas, Design and analysis of a hybrid radio frequency and visible light communication system, *IEEE Trans. Commun.* 65 (10) (2017) 4334–4347.
- [11] S. Shao, A. Kheishah, M. Ayyash, M.B. Rahaim, H. Elgala, V. Jungnickel, S. D., T.D.C. Little, J. Hilt, R. Freund, Design and analysis of a visible-light-communication enhanced wifi system, *J. Opt. Commun. Netw.* 7 (10) (2015) 960–973.
- [12] Z. Li, S. Shao, A. Kheishah, M. Ayyash, I. Abdalla, H. Elgala, M. Rahaim, T. Little, Design and implementation of a hybrid RF-VLC system with bandwidth aggregation, in: Int. Wireless Communications Mobile Computing Conf., Limassol, Cyprus, June 2018 pp. 194–200.
- [13] H. Liu, L. Zhang, A medium access scheme with dynamic contention window-based successive transmission for visible light communications system, in: Int. Conf. on Information and Communication Tech. Convergence, Jeju, South Korea, October 2016, pp. 499–504.
- [14] M. Hammouda, S. Akin, A.M. Vegni, H. Haas, J. Peissig, Link selection in hybrid RF/VLC systems under statistical queuing constraints, *IEEE Trans. Wireless Commun.* 17 (4) (2018) 2738–2754.
- [15] Y.C. Hsiao, C.M. Chen, C. Lin, Energy efficiency maximization in multi-user miso mixed RF/VLC heterogeneous cellular networks, in: 2018 15th Annual IEEE International Conference on Sensing, Communication, and Networking (SECON), Hong Kong, China, June 2018.
- [16] M. Kafafy, Y. Fahmy, M. Abdallah, M. Khairy, Power efficient downlink resource allocation for hybrid RF/VLC wireless networks, in: 2017 IEEE Wireless Communications and Networking Conference (WCNC), March 2017, San Francisco, CA, USA.
- [17] N. Le, Y.M. Jang, Broadcasting MAC protocol for IEEE 802.15.7 visible light communication, in: Fifth Int. Conference on Ubiquitous and Future Networks, ICUFN, July 2013, Da Nang, Vietnam pp. 667–671.
- [18] N. Le, S. Choi, Y.M. Jang, Cooperative MAC protocol for LED-ID systems, in: ICTC 2011, Seoul, South Korea, Sept. 2011, pp. 144–150.
- [19] B. Xu, M. Zhang, Y. Sha, Design of Media Access Control in visible light communication system and a simple way to avoid dual transmit over dual Access Point, in: 15th Int. Conference on Optical Communications and Networks, ICOON, Hangzhou, China, September 2016.
- [20] H. Liu, L. Zhang, M. Jiang, Energy efficient medium access scheme for visible light communication system based on IEEE 802.15.7 with unsaturated traffic, *IET Commun.* 10 (18) (2016) 2534–2542.
- [21] Q. Mao, P. Yue, M. Xu, Y. Ji, Z. Cui, OCTMAC: A VLC based MAC protocol combining optical CDMA with TDMA for VANETS, in: 2017 International Conference on Computer, Information and Telecommunication Systems, CITS, Dalian, China, July 2017. pp. 234–238.
- [22] N.-T. Le, Y.M. Jang, Resource allocation for multichannel broadcasting visible light communication, *Opt. Commun.* 355 (2015) 451–461.
- [23] Z. Wang, Y. Liu, Y. Lin, S. Huang, Full-duplex MAC protocol based on adaptive contention window for visible light communication, *IEEE/OSA J. Opt. Commun. Networking* 7 (3) (2015) 164–171, <http://dx.doi.org/10.1364/JOCN.7.000164>.
- [24] D.L. Msongaleli, K. Küçük, A. Kavak, Adaptive polling medium access control protocol for optic wireless networks, *Appl. Sci.* 9 (6) (2019).
- [25] H. Marshoud, V.M. Kapinas, G.K. Karagiannidis, S. Muhaiddat, Non-orthogonal multiple access for visible light communications, *IEEE Photonics Technol. Lett.* 28 (1) (2016) 51–54.
- [26] D. Msongaleli, K. Küçük, Dynamic future knowledge maximum transmission unit (DFK-MTU) for optic wireless networks, in: 26th Signal Processing and Communications Applications Conf. (SIU), 2018, <http://dx.doi.org/10.1109/SIU.2018.8404326>.
- [27] G. G. Bianchi, Performance analysis of the IEEE 802.11 distributed coordination function, *IEEE J. Sel. Areas Commun.* 18 (3) (2000) 535–547.
- [28] P. Shams, M. Erol-Kantarci, M. Uysal, MAC layer performance of the IEEE 802.15.7 visible light communication standard, *Trans. Emerg. Telecommun. Technol.* 27 (5) (2016) 662–674, <http://dx.doi.org/10.1002/ett.3015>.
- [29] A. Vavoulas, H.G. Sandalidis, T.A. Tsiftsis, N. Vaopoulos, Coverage aspects of indoor VLC networks, *J. Lightwave Technol.* 33 (23) (2015) 4915–4921, <http://dx.doi.org/10.1109/JLT.2015.2492420>.
- [30] A. Alshanyour, A. Agarwal, Three-Dimensional Markov Chain Model for Performance Analysis of the IEEE 802.11 Distributed Coordination Function, in: IEEE GLOBECOM, HI, USA, Nov. 2009.
- [31] K. Küçük, SA-MAC: NS3 codes for self-adaptive medium access control protocol for aggregated VLC-RF wireless networks, 2020, <http://dx.doi.org/10.6084/m9.figshare.9983393>, [retrieved 29 Jan. 2020] figshare.
- [32] Q. Wang, D. Giustiniano, Intra-frame bidirectional transmission in networks of visible LEDs, *IEEE/ACM Trans. Netw.* 24 (6) (2016) 3607–3619.